The pair correlation function for a generalized ballistic deposition model

1996 J. Phys. A: Math. Gen. 29 2309

(http://iopscience.iop.org/0305-4470/29/10/011)

J. Phys. A: Math. Gen. **29** (1996) 2309–2324. Printed in the UK

The pair correlation function for a generalized ballistic deposition model

D Boyer, G Tarjus and P Viot

Laboratoire de Physique Théorique des Liquides, Université Pierre et Marie Curie, 4 place Jussieu, 75252 Paris Cedex 05, France

Received 11 January 1996

Abstract. The disordered structure formed by particles that are sequentially deposited onto a line is analysed. Analytical expressions of the pair correlation function, the structure factor, and the fluctuations of the number of particles are obtained for the generalized ballistic deposition model. For all integer values of the distance between particles, the pair correlation function has a discontinuity and a delta-singularity, which both result from cluster formation. A comparison is made with equilibrium configurations of sticky hard rods. It is shown that, in contrast to equilibrium systems (but as in the random sequential addition model), the correlations between particles decay faster than exponentially at large distances.

1. Introduction

Adsorption of macromolecules such as proteins and colloidal particles at liquid–solid interfaces often occurs irreversibly [1, 2]. Diffusion on the surface and desorption are indeed typically slow compared to experimental times. The adsorbed layer that is generated in such processes appears as a disordered non-equilibrium configuration of particles [1, 3]. Several experimental results have been interpreted in terms of the random sequential addition (RSA) model [1, 2]. In this latter model, hard particles are deposited randomly, one after another, on a surface. If no overlap occurs with pre-adsorbed particles, the trial particle is clamped on the surface; otherwise, it is rejected and a new attempt is made [4]. This model accounts for irreversibility and many-body exclusion effects, and it provides a good description of adsorption experiments in which the diffusive motions of the particles in solution, together with hydrodynamic forces, lead to a randomization of the deposition process [5–7]. However, for heavy colloidal particles, gravitational effects cannot be ignored [8]. Talbot and Ricci [9] have proposed a ballistic deposition model in which particles follow straight-line trajectories in solution and paths of steepest descent on previously adsorbed particles. As multilayer formation is prevented, a particle which is trapped in an elevated position is immediately removed. As a generalization which allows one to study all intermediate situations between RSA and ballistic deposition, Viot *et al* [10] have introduced a model in which the relative efficiency of the adsorption by direct deposition and by rolling on pre-adsorbed particles is controlled by a tuning parameter a. The model leads to cluster formation and, in $(1+1)$ dimensions, the time evolution of the particle and cluster densities can be obtained exactly [10]. In $(2+1)$ dimensions, this generalized ballistic deposition model has been investigated by computer simulation and density expansions. The configurations are formed by clusters of different sizes [11, 12]; a percolation transition

0305-4470/96/102309+16$19.50

occurs for a finite value of a ($a \sim 3$), i.e. when the restructuring effect due to the rolling mechanism becomes efficient enough [13].

To characterize these non-equilibrium processes, the knowledge of the adsorption kinetics (by which one means the time dependence of the density) may not be sufficient and an analysis of the spatial correlations appears as a way to significantly improve the understanding of the adsorption mechanism. Such a study has been performed by Wojtaszczyk *et al* [8], who have been able to obtain the radial distribution function of colloidal particles adsorbed on mica by using image analysis techniques. There is, thus, a great interest in developing theoretical studies of spatial correlations. An exact expression for the pair correlation function has been derived for the RSA of dimers of one-dimensional (1D) lattices [14–17] and more recently for the RSA of k-mers and its continuum limit known as the car parking problem [18]. In higher dimensions, the pair correlation function can be obtained either by computer simulations or by solving approximate integral equations [19].

In this paper, we derive an exact expression for the pair correlation function of the $(1 + 1)$-dimensional version of the generalized ballistic deposition (GBD) model. It is obtained as the solution of a set of rate equations that can be written in a closed form thanks to the 'gap-Markov' shielding property [20]. With the explicit expression of the pair correlation function in hand, we obtain a formula for the fluctuations of the number of particles. This quantity is an important experimental signature of the nature of the deposition process [8]. We discuss the influence of the tuning parameter a on the correlations. Finally, we present a comparison with the equilibrium fluid of sticky rods.

2. Kinetics

In one dimension, the GBD model is defined as follows. Hard disks of diameter σ are deposited onto an infinite line sequentially, uniformly, and at a constant rate, k, per unit length. If, at time τ, the new disk does not encounter any pre-adsorbed disk, it adsorbs with a probability p. Otherwise, it rolls over one or several pre-adsorbed disks by following the path of steepest descent; if it eventually reaches the line, the new disk is accepted with a probability p' and if not, it is rejected (no multi-layer formation is allowed in this model). Using dimensionless variables, $t = \sigma k p \tau$, $h = l/\sigma$, $a = p'/p$, one can see that for $a = 0$, no particles are adsorbed after rolling over pre-adsorbed particles, which corresponds to an RSA process, whereas for $a = 1$, we recover the ballistic deposition model of Talbot and Ricci [9]. In the limit $a \to +\infty$, only deposition via rolling is permitted after a first seed particle is inserted, and this results in a close-packed configuration. The parameter a is thus a measure of the efficiency of the rolling mechanism. The interest of this generalized version of ballistic deposition model is that it allows a non-negligible fraction of those particles rolling over pre-adsorbed particles to be rejected, which seems to be a reasonable physical assumption for monolayer formation.

If $\rho(t)$ denotes the number density of particles on the line at time t, its time evolution in the GBD model is governed by the following rate equation:

$$\frac{\mathrm{d}\rho(t)}{\mathrm{d}t} = P(l = 1, t) + 2a P_1(l = 1, t) \tag{1}$$

where $P(l, t)$ is the probability of finding a cavity (i.e. an empty interval of diameter *at least* l) and $P_1(l, t)$ is the probability of finding a cavity of length *at least* l bounded on at least one side by a particle.

To determine $P(l, t)$ and $P_1(l, t)$, one notes that a cavity of diameter $l \geqslant 1$ can be

destroyed by inserting particles that can either lie completely within this cavity or can partially overlap the right or the left sides of the cavity. The time evolution of the probability function $P(l,t)$ can then be expressed as

$$-\frac{\partial P(l,t)}{\partial t} = (l-1)P(l,t) + 2\int_0^1 \mathrm{d}u\, P(l+u,t) + 2a\int_0^1 \mathrm{d}u\, P_1(l+u,t) \qquad \text{for } l \geqslant 1. \tag{2}$$

Moreover, $P(l,t)$ and $P_1(l,t)$ are related by the following sum rule:

$$P(l,t) = \int_l^{+\infty} \mathrm{d}u\, P_1(u,t). \tag{3}$$

Looking for a solution of the type $P(l,t) = h_a^2(t)\exp(-(l-1)t)$ for $l \geqslant 1$ and using the initial condition $P(l,t=0) = 1$, the solution of equation (2) comes as

$$h_a(t) = \exp\left(-\int_0^t \frac{1-\mathrm{e}^{-u}}{u}\,\mathrm{d}u + a(1-t-\mathrm{e}^{-t})\right). \tag{4}$$

The number density of particles is then equal to

$$\rho(t) = \int_0^t \mathrm{d}t_1\,(1+2at_1)h_a^2(t_1). \tag{5}$$

This result has already been derived by Viot *et al* [10] using an approach in terms of gap distribution functions. Notice that the saturation state is reached exponentially, $\rho(\infty) - \rho(t) \sim \exp(-2at)/(at)$, for all non-zero values of a, whereas for $a = 0$ (corresponding to the car parking problem), the asymptotic kinetics is algebraic, $\rho(\infty) - \rho(t) \sim 1/t$.

3. Pair correlation function

To obtain the pair correlation function, one must write kinetic equations for higher-order correlation functions. Let $(l+1)$ denote the centre-to-centre distance between two adsorbed particles; $\rho^2 g(l+1)\,\mathrm{d}l$ is the probability density of finding two particle centres that are separated by a distance $(l+1)$. Hard core interactions which prevent particle overlap impose that the pair correlation function satisfies $g(l+1) = 0$ for $(l+1) < 1$. Between t and $t + \mathrm{d}t$, new pairs of particles are created by the insertion of a particle at a given point **1** which is at a distance $(l+1)$ of a pre-adsorbed particle centred on **2**, or by the insertion of a particle at point **2** provided that a pre-adsorbed particle is centred on the point **1** [21]. The time evolution of the pair correlation function is then given by

$$\begin{aligned}\frac{\partial \rho^2(t)g(l+1,t)}{\partial t} &= 2[Q_1(l_1=1,l,t) + aH(l-1)Q_2(l_1=1,l-1,t) \\ &\quad + aQ_3(l_1=1,l,t) + a\delta(l)P_1(l,t)]\end{aligned} \tag{6}$$

where H denotes the Heaviside step function; $Q_1(l_1,l,t)$ is the probability of finding a cavity of diameter *at least* l_1 whose centre is at a distance $(l + (l_1+1)/2)$ (to the right or to the left) of the centre of a pre-adsorbed particle, $Q_2(l_1,l,t)$ is the probability of finding a cavity of diameter *at least* l_1 bounded on one side by a pair of particles whose centres are separated by a distance $(l+1)$, and $Q_3(l_1,l,t)$ is the probability of finding a cavity of diameter *at least* l_1 bounded on one side by a particle and such that there is a particle on the other side whose centre is at a distance $(l+l_1+1)$ from the other particle centre. The

Q-functions are schematically represented in figure 1(a). Similarly to equation (3), there exists a sum rule between $Q_1(l_1, l, t)$ and $Q_3(l_1, l, t)$ that can be written

$$Q_1(l_1, l, t) = \int_{l_1}^{+\infty} \mathrm{d}u \; Q_3(u, l, t). \tag{7}$$

The rate equations for $Q_1(l_1, l, t)$ and $Q_2(l_1, l, t)$ are derived by considering all possible ways of destruction or creation of a pair particle–cavity. The rules of evolution are the following: a cavity can only be destroyed, either by partial overlap by an incoming particle (arrived by direct deposition or by rolling over a neighbouring particle) or by complete insertion of an incoming particle (by direct deposition only); a particle can only be added, either by direct deposition or by rolling over neighbouring particles. The rate equations for the particle–cavity Q-functions involve then three different cavity–cavity functions which are denoted $P_i(l_1, l, l_2, t)$, $i = 1, 2, 3$, and are represented in figure 1(b). The rate equations for the P-functions can be similarly derived, and it is easy to verify that no higher-order correlation functions are involved. This a consequence of the 'gap-Markov' shielding property that is valid for sequential deposition processes [4]: a gap (or empty interval) of length at least one completely shields from each other the two semi-infinite regions of the line that are to the left and the right, in the sense that any filling event in one region is not affected by the state of the other region. Noting also that for $0 \leqslant l < 1$ an interval must be empty, it follows that $Q_1(l_1, l, t) = P_1(l_1 + l, t)$, $P_1(l_1, l, l_2, t) = P(l_1 + l + l_2, t)$, $P_2(l_1, l, l_2, t) = P_1(l_1 + l + l_2, t)$, $P_3(l_1, l, l_2, t) = P_2(l_1 + l + l_2, t)$ for $0 \leqslant l < 1$. $P_2(l, t)$ is the probability of finding a cavity of diameter l bounded on both sides by particles. We then obtain a closed set of equations for the pair correlation function.

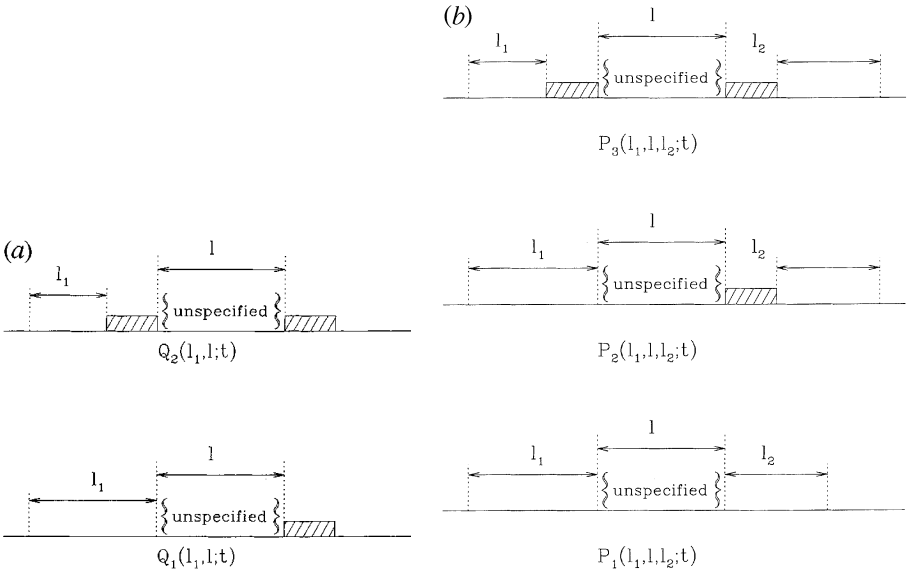

Figure 1. Schematic representation of the particle–cavity Q-functions (a) and cavity–cavity P-functions (b).

Using again the 'gap-Markov' shielding property, we write $P_i(l_1, l, l_2, t) = h_a^2(t)\, p_i(l, t) \exp[-(l_1 + l_2 - 2)t]$ for $l_1 \geqslant 1$, $l_2 \geqslant 1$, $i = 1, 2, 3$, and $Q_i(l_1, l, t) = h_a(t) q_i(l, t) \exp[-(l_1 - 1)t]$ for $l_1 \geqslant 1$ and $i = 1, 2$. The rate equation for the pair

correlation function is then by given by

$$\rho^2 g(l+1,t) = 2\int_0^t \mathrm{d}t_1\, h_a(t_1)((1+at_1)q_1(l,t_1) + aq_2(l,t_1) + at_1 h_a(t_1)\delta(l)) \tag{8}$$

where $q_1(l,t)$ and $q_2(l,t)$ obey the following equations:

$$\begin{aligned}\frac{\partial q_1(l,t)}{\partial t} = &-\int_0^{\mathrm{Min}(1,l)} \mathrm{d}u\, \mathrm{e}^{-ut} q_1(l-u,t) - a(1-H(l-1))q_1(l,t)\\ &-aH(l-1)\int_0^{\mathrm{Min}(1,l-1)} \mathrm{d}u\, \mathrm{e}^{-ut} q_2(l-1-u,t) + h_a(t)(1+at)p_1(l,t)\\ &+aH(l-1)h_a(t)p_2(l-1,t)\end{aligned} \tag{9}$$

$$\begin{aligned}\frac{\partial q_2(l,t)}{\partial t} = &\,\mathrm{e}^{-t} q_1(l,t) - aq_2(l,t) + aH(l-1)q_2(l-1,t)\mathrm{e}^{-t} + (1+at)h_a(t)p_2(l,t)\\ &+aH(l-1)h_a(t)p_3(l-1,t) + a\delta(l)(h_a(t)p_2(t) + q_1(l)\mathrm{e}^{-t}).\end{aligned} \tag{10}$$

Similarly, we have for the functions $p_i(l,t)$:

$$\begin{aligned}\frac{\partial p_1(l,t)}{\partial t} = &-2\int_0^{\mathrm{Min}(1,l)} \mathrm{d}u\, \mathrm{e}^{-ut} p_1(l-u,t)\\ &-2aH(l-1)\int_0^{\mathrm{Min}(1,l-1)} \mathrm{d}u\, \mathrm{e}^{-ut} p_2(l-1-u,t) - (1-\mathrm{Min}(1,l))\mathrm{e}^{-(l+1)t}\end{aligned} \tag{11}$$

$$\begin{aligned}\frac{\partial p_2(l,t)}{\partial t} = &\,\mathrm{e}^{-t} p_1(l,t) - ap_2(l,t) - a(1-H(l-1))p_2(l,t) + aH(l-1)\mathrm{e}^{-t} p_2(l-1,t)\\ &-\int_0^{\mathrm{Min}(1,l)} \mathrm{d}u\, \mathrm{e}^{-ut} p_2(l-u,t)\\ &-aH(l-1)\int_0^{\mathrm{Min}(1,l-1)} \mathrm{d}u\, \mathrm{e}^{-ut} p_3(l-1-u,t)\end{aligned} \tag{12}$$

$$\frac{\partial p_3(l,t)}{\partial t} = 2\mathrm{e}^{-t} p_2(l,t) - 2ap_3(l,t) + 2aH(l-1)\mathrm{e}^{-t} p_3(l-1,t) + 2a\delta(l)p_2(l)\mathrm{e}^{-t}. \tag{13}$$

Taking the spatial Laplace transform, the above equations can be expressed in a more compact matrix form. With the following definitions, $\tilde{p}_i(s,t) = \int_0^{+\infty} \mathrm{d}l\, \mathrm{e}^{-sl} p_i(l,t)$, $\tilde{q}_i(s,t) = \int_0^{+\infty} \mathrm{d}l\, \mathrm{e}^{-sl} q_i(l,t)$, and $\tilde{g}(s,t) = \int_0^{+\infty} \mathrm{d}l\, \mathrm{e}^{-sl} g(l+1,t)$ (note that for convenience we choose to shift the Laplace transform of $g(l,t)$), equations (8)–(13) can be rewritten as

$$\frac{\partial \rho^2(t)\tilde{g}(s,t)}{\partial t} = 2h_a(t)[(1+at)\tilde{q}_1(s,t) + a\mathrm{e}^{-s}\tilde{q}_2(s,t) + ath_a(t)] \tag{14}$$

$$\begin{aligned}\frac{\partial}{\partial t}\begin{pmatrix}\tilde{q}_1(s,t)\\ \tilde{q}_2(s,t)\end{pmatrix} = &\begin{pmatrix}-A(s,t) & -a\mathrm{e}^{-s}A(s,t)\\ \mathrm{e}^{-t} & -a(t+s)A(s,t)\end{pmatrix}\begin{pmatrix}\tilde{q}_1(s,t)\\ \tilde{q}_2(s,t)\end{pmatrix}\\ &+\begin{pmatrix}(1+at)h_a(t)\tilde{p}_1(s,t) + ah_a(t)\mathrm{e}^{-s}\tilde{p}_2(s,t) - ath_a(t)A(s,t)\\ (1+at)h_a(t)\tilde{p}_2(s,t) + ah_a(t)\mathrm{e}^{-s}\tilde{p}_3(s,t) + ah_a(t)(t\mathrm{e}^{-t} + C(a,t))\end{pmatrix}\end{aligned} \tag{15}$$

$$\begin{aligned}\frac{\partial}{\partial t}\begin{pmatrix}\tilde{p}_1(s,t)\\ \tilde{p}_2(s,t)\\ \tilde{p}_3(s,t)\end{pmatrix} = &\begin{pmatrix}-2A(s,t) & -2a\mathrm{e}^{-s}A(s,t) & 0\\ \mathrm{e}^{-t} & -(1+a(t+s))A(s,t) & -a\mathrm{e}^{-s}A(s,t)\\ 0 & 2\mathrm{e}^{-t} & -2a(t+s)A(s,t)\end{pmatrix}\begin{pmatrix}\tilde{p}_1(s,t)\\ \tilde{p}_2(s,t)\\ \tilde{p}_3(s,t)\end{pmatrix}\\ &+\begin{pmatrix}-\mathrm{e}^{-t}B(s,t)\\ -aA(s,t)C(a,t)\\ 2a\mathrm{e}^{-t}C(a,t)\end{pmatrix}\end{aligned} \tag{16}$$

where

$$A(s,t) = \frac{1-\mathrm{e}^{-(s+t)}}{s+t} \tag{17}$$

$$B(s,t) = \frac{1}{s+t} - \frac{1-\mathrm{e}^{-(s+t)}}{(s+t)^2} \tag{18}$$

and

$$C(a,t) = \frac{\mathrm{e}^{-2at} - \mathrm{e}^{-2t}}{2(1-a)}. \tag{19}$$

To solve these coupled equations, we first introduce the following variables: $q_1(s,t)$, $(\mathrm{e}^{-s}/(t+s))q_2(s,t)$, $p_1(s,t)$, $(\mathrm{e}^{-s}/(t+s))p_2(s,t)$, $(\mathrm{e}^{-s}/(t+s))^2 p_3(s,t)$. The matrices can now be made upper triangular in a basis that is independent of time. To do so, one can choose the following linear combinations of the new variables: $X_1(s,t) = q_1(s,t)$, $X_2(s,t) = (\mathrm{e}^{-s}/(t+s))q_2(s,t) - q_1(s,t)$, $Y_1(s,t) = p_1(s,t)$, $Y_2(s,t) = (\mathrm{e}^{-s}/(t+s))p_2(s,t) - p_1(s,t)$, $Y_3(s,t) = (\mathrm{e}^{-s}/(t+s))^2 p_3(s,t) - 2(\mathrm{e}^{-s}/(t+s))p_2(s,t) + p_1(s,t)$. The differential equations for the functions X_2, Y_2, and Y_3 can be explicitly solved and the rate equation for the pair distribution function can be re-expressed as (see appendix A for details)

$$\frac{\partial \rho^2 \tilde{g}(s,t)}{\partial t} = 2h_a(t)((1+a(2t+s))X_1(s,t)) \tag{20}$$

$$\frac{\partial}{\partial t}X_1(s,t) = -A(s,t)(1+a(t+s))X_1(s,t) + h_a(t)((1+a(2t+s))Y_1(s,t) - a\mathrm{e}^{-t}) \tag{21}$$

$$\frac{\partial}{\partial t}Y_1(s,t) = -2A(s,t)(1+a(t+s))Y_1(s,t) + (2aA(s,t) - B(s,t))\mathrm{e}^{-t}. \tag{22}$$

It is possible to calculate $g(l+1,t)$ for successive intervals using the property that the solution of equations (8)–(13) is obtainable by expanding the functions on the basis $\{H(l-n)(l-n)^{m-1}/(m-1)!\exp(-(l-n)t)\}$ for $m \geqslant 1$ and $\{\delta(l-n)\exp(-(l-n)t)\}$ for $n \geqslant 0$. Details of the calculation are given in appendix B. For $0 \leqslant l < 1$, one obtains

$$g(l+1,t) = \frac{2}{\rho^2(t)}\int_0^t \mathrm{d}t_1\, h_a^2(t_1)(t_1(1+at_1)\mathrm{e}^{-lt_1} + at_1\delta(l)). \tag{23}$$

It is worth noting that the logarithmic divergence at contact of the pair correlation at saturation is only obtained for $a = 0$. For any non-zero value of a, the pair correlation function at contact is finite even at saturation, provided the singular delta contribution is removed. For $1 \leqslant l < 2$, one obtains

$$\begin{aligned} g(l+1,t) = {} & \frac{2}{\rho^2(t)}\int_0^t \mathrm{d}t_1\, t_1(1+at_1)h_a^2(t_1)\mathrm{e}^{-lt_1} \\ & + \frac{2}{\rho^2(t)}\int_0^t \mathrm{d}t_1\, h_a(t_1)\mathrm{e}^{-at_1}\int_0^{t_1}\mathrm{d}t_2\, \mathrm{e}^{at_2}h_a(t_2)[a^2(C(a,t_2)+t_2\mathrm{e}^{-t_2})\delta(l-1) \\ & + a(1+at_1)\mathrm{e}^{-(l-1)t_1}(C(a,t_2)+t_2\mathrm{e}^{-t_2}) \\ & + a((1+at_2)C(a,t_2)+t_2\mathrm{e}^{-t_2})\mathrm{e}^{-(l-1)t_2} \\ & + (1+at_1)((1+at_2)C(a,t_2)+t_2\mathrm{e}^{-t_2})\frac{\mathrm{e}^{-(l-1)t_2}-\mathrm{e}^{-(l-1)t_1}}{t_1-t_2}. \end{aligned} \tag{24}$$

For larger distances, the calculation rapidly becomes tedious and leads to rather lengthy expressions. A striking feature of the pair correlations is the existence of an infinite set of

delta singularities at all integer values of l. The amplitudes of these singularities are given by

$$g^s(n+1,t) = \frac{1}{\rho^2(t)}\frac{2a^{n+1}}{(n-1)!}\int_0^t \mathrm{d}t_1\, h_a(t_1)\mathrm{e}^{-at_1}\int_0^{t_1}\mathrm{d}t_2\, h_a(t_2) \times\Bigg[t_2\mathrm{e}^{-(1-a)t_2}(\mathrm{e}^{-t_2}-\mathrm{e}^{-t_1})^{n-1} +\mathrm{e}^{-at_2}\int_0^{t_2}\mathrm{d}t_3\,(2\mathrm{e}^{-t_3}-\mathrm{e}^{-t_1}-\mathrm{e}^{-t_2})^{n-1}\mathrm{e}^{-2(1-a)t_3}\Bigg]. \tag{25}$$

At short times, these amplitudes increase as

$$g^s(n+1,t) \sim \frac{2a^{n+1}}{(n+1)!}t^{n+2}. \tag{26}$$

This result, equation (26), can be understood by noting that the singular correlation between a pair of particles at a distance $n+1$ requires the appearance of a connected cluster of size $n+1$. From equation (25), one can also deduce by using Laplace's method the asymptotic behaviour for large distances; at saturation, it is given by

$$g^s(n,\infty) \sim \frac{(2a)^n}{n!n^{4a}}. \tag{27}$$

A superexponential decay with distance (i.e. with n) is thus observed for the singularities, which means that the spatial correlations between two particles belonging to the same cluster decrease very rapidly. This fast decrease of the correlations is related to the absence of very large clusters (note that the absence of cluster–cluster coalescence in 1D cooperative sequential processes prevents the formation of large clusters) [14].

Concerning the regular part of the pair correlation function, one observes that there are finite discontinuities at all non-zero integer values of the distance between two particles. An analytical expression of these discontinuities can be obtained by using the recursion equations given in appendix B. For example, one has for $\Delta g(2,t) = g(2^+,t) - g(2^-,t)$,

$$\Delta g(2,t) = 2a\int_0^t \mathrm{d}t_1\, h_a(t_1)\mathrm{e}^{-at_1}\int_0^{t_1}\mathrm{d}t_2\,\mathrm{e}^{at_2}h_a(t_2)((2+t_1)\mathrm{e}^{-t_2}+(2+a(t_1+t_2))C(a,t_2)). \tag{28}$$

The discontinuity is an increasing function of time and vanishes when a goes to zero. Similar results can be obtained for discontinuities at larger integer values of the distance, and one shows that the asymptotic behaviour for large distances is superexponentially decreasing like the singulairities (see equation (27)).

To obtain an explicit expression for the Laplace transform of the pair correlation function $\tilde{g}(s,t)$, one integrates equations (20)–(22) with the initial conditions $X_1(s,0)=0$, $Y_1(s,0)=1/s$, which gives

$$Y_1(s,t) = h_a^2(t+s)\left[\frac{1}{sh_a^2(s)} + \int_0^t \mathrm{d}t_1\,\frac{2aA(s,t_1)-B(s,t_1)}{h_a^2(t_1+s)}\mathrm{e}^{-t_1}\right] \tag{29}$$

$$X_1(s,t) = h_a(t+s)\int_0^t \mathrm{d}t_1\,\frac{h_a(t_1)}{h_a(t_1+s)}[-a\mathrm{e}^{-t_1}+(1+a(2t_1+s))Y_1(s,t_1)]. \tag{30}$$

Inserting equations (29) and (30) in equation (20) yields

$$\rho^2(t)\tilde{g}(s,t) = \frac{1}{s}\left[\int_0^t \mathrm{d}t_1\,(1+a(2t_1+s))\frac{h_a(t_1)h_a(t_1+s)}{h_a(s)}\right]^2$$

$$+2\int_0^t \mathrm{d}t_1\,(1+a(2t_1+s))h_a(t_1)h_a(t_1+s)$$
$$\times\int_0^{t_1}\mathrm{d}t_2\left[-\frac{h_a(t_2)}{h_a(t_2+s)}a\mathrm{e}^{-t_2}+(1+a(2t_2+s))h_a(t_2)h_a(t_2+s)\right.$$
$$\left.\times\int_0^{t_2}\mathrm{d}t_3\,\frac{\mathrm{e}^{-t_3}}{h_a^2(t_3+s)}(2aA(s,t_3)-B(s,t_3))\right]. \tag{31}$$

Noting that as $s\to 0$, $\tilde{g}(s,t)\to 1/s$, and using the Tauberian theorem, we obtain that, as expected, $g(l+1,t)\to 1$ when $l\to+\infty$. By taking the inverse Laplace transform, the above formula, equation (31), provides a tractable way to calculate the pair correlation function. Figure 2(a) shows the pair correlation function $g(l,\infty)$ at saturation for various values of the parameter a. When a becomes larger, $g(l+1,\infty)$ is more structured: the amplitudes of the singularities and of the discontinuities, as well as the range of the correlations, increase with a. Indeed, when a gets bigger, the deposition by rolling on pre-adsorbed disks becomes more efficient and clusters of larger sizes are formed. Figure 2(b) displays the pair correlation function $g(l,\rho)$ for $a=1$ and for various values of the density. Note that the amplitude of the first singularity decreases when ρ increases, whereas all others decrease when ρ increases: this comes from the fact that dimer formation is not prevented at the early stages of the process whereas trimer and k-mer formation requires two or more pre-adsorbed particles.

For a small increase of a, the saturation density is only slightly changed, whereas the local structure is significantly altered. Analysing the structure of the deposited layer then allows a better characterization of the nature of the deposition process than monitoring the adsorption kinetics or measuring the saturation density.

4. Fluctuations

The static structure factor $S(k,t)$ is another quantity of interest which permits one to investigate the structure of the adsorbed layer. $S(k,t)$ can be deduced from equation (31) by the relation

$$S(k,t)=1+2\rho(t)\,\mathrm{Re}\left\{\left(\lim_{\epsilon\to 0}\left(\tilde{g}(s,t)\mathrm{e}^{-s}-\frac{1}{s}\right)\Big|_{s=\epsilon+\mathrm{i}k}\right)\right\}. \tag{32}$$

Figure 3 displays the static structure factor for various values of a at saturation. For any non-zero value of a, the presence of delta-peaks in the pair correlation function leads to periodic oscillations in $S(k,t)$ that provide another signature of cluster formation in the deposition process. It is worth noting that these strong oscillations of the structure factor do not correspond to the apperance of a long-range structure, since the correlations between particles have a superexponential decay.

The variance of the number of particles is a macroscopic quantity which also gives some information on the nature of the adsorption or deposition mechanism. In recent experiments, the fluctuations have been obtained by statistical analysis of a large number of samples that are formed by particles adsorbed on a finite surface [8]. They have been shown to give a simple way to discriminate between different models of the adsorption process. Since the deposition process is uniform, the fluctuation theorem is still valid [19] and one has

$$\frac{\langle\Delta N^2\rangle}{\langle N\rangle}=S(k=0,t). \tag{33}$$

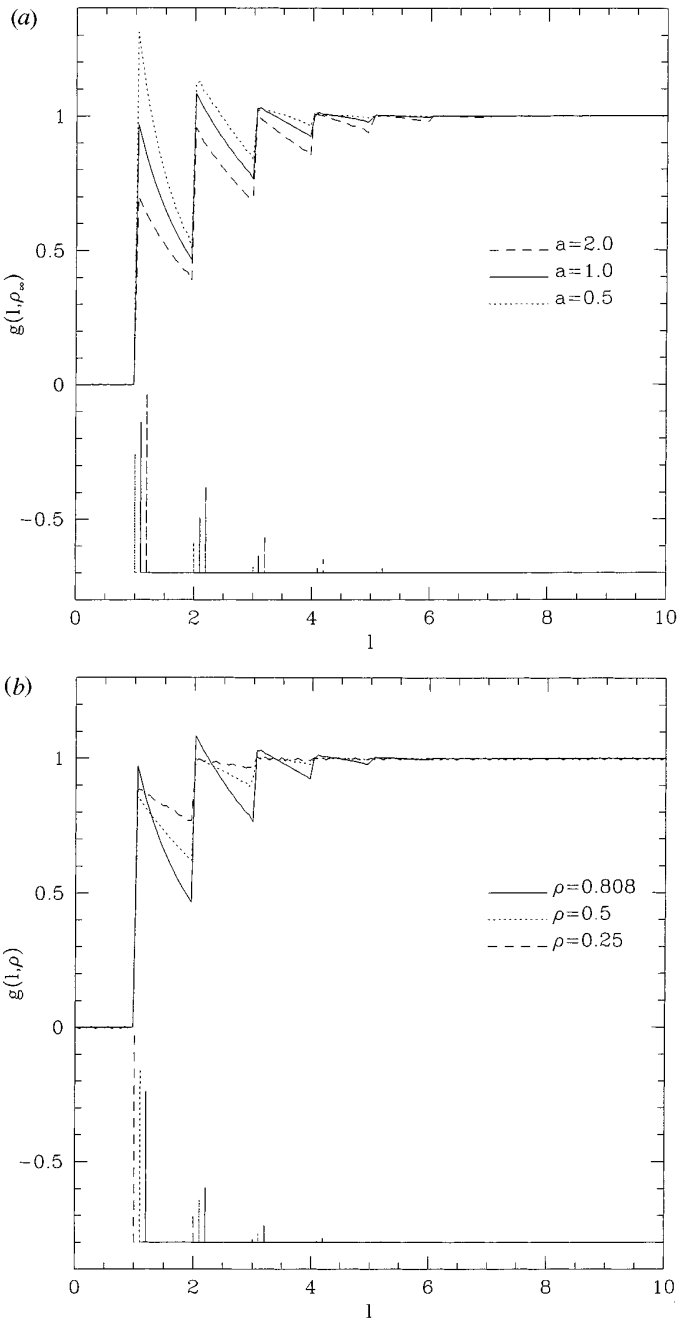

Figure 2. (*a*) Pair correlation function $g(l, \rho_\infty)$ at saturation for $a = 0.5, 1.0, 2.0$. The curve corresponds to the regular part of $g(l, \rho_\infty)$. The vertical straight lines correspond to the amplitudes of the delta-singularities; for clarity, they are all shifted downwards by -0.7 from the baseline and those for $a = 1$ and $a = 2$ are shifted to the right by 0.1 and 0.2, respectively. (*b*) Pair correlation function $g(l, \rho)$ for $\rho = 0.25, 0.5, 0.808$. The curve corresponds to the regular part of $g(l, \rho)$. The vertical straight lines correspond to the amplitudes of the delta-singularities; they are all shifted downwards by -0.8 from the baseline and those for $\rho = 0.5$ and $\rho = 0.808$ are shifted to the right by 0.1 and 0.2, respectively.

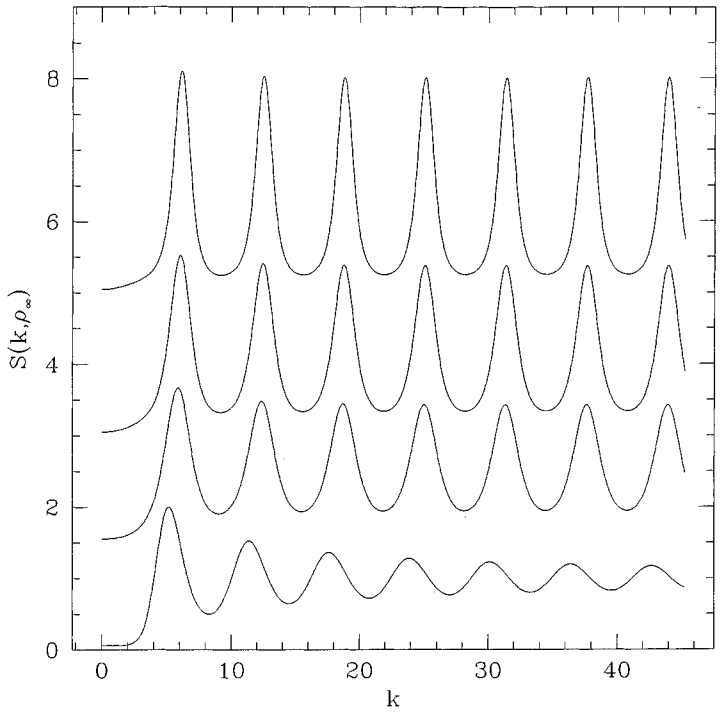

Figure 3. Static structure factor $S(k,\rho)$ are displayed for various values of a at saturation: from bottom to top, $a = 0, 0.5, 1.0, 2.0$; the latter three are shifted upwards by 1.5, 3, 4.5, respectively.

Note that the above quantity only requires the knowledge of the pair correlations, in contrast to the available surface function which is in principle expressed in terms of all n-particle densities.

Inserting equations (31) and equation (32) in equation (33) yields

$$\frac{\langle \Delta N^2 \rangle}{\langle N \rangle} = 1 + 2\rho(t) + 2\dot{\rho}(t) + \frac{4}{\rho(t)}\left[\int_0^t \mathrm{d}t_1\, a\dot{\rho}(t_1)(\mathrm{e}^{-t_1} - 1) + \int_0^t \mathrm{d}t_1 \int_0^{t_1} \mathrm{d}t_2\, \dot{\rho}(t_1)\dot{\rho}(t_2) \int_0^{t_2} \mathrm{d}t_3\, \frac{\mathrm{e}^{-t_3}}{h_a^2(t_3)}(2aA(t) - B(t_3)) \right] \tag{34}$$

where $\dot{\rho}(t) = (1 + 2at)h_a^2(t)$ denotes the time derivative of $\rho(t)$. We show in figure 4 the variance of the number of particles versus density for different values of a. For any given density, the variance is an increasing function of a. When a=1, which corresponds to the simple ballistic deposition model, the slope of the curve is equal to zero at $\rho = 0$. This feature is valid in all dimensions and it is much more pronounced in two dimensions where the two first orders of the density expansion vanish when $a = 1$ [12].

5. Comparison with the fluid of sticky rods

It is easy to realize that the (1+1)-dimensional generalized ballistic deposition model can be reduced to a sequential adsorption process on a one-dimensional substrate. Instead of being random, i.e. governed only by exclusion effects due to the non-overlap constraint between

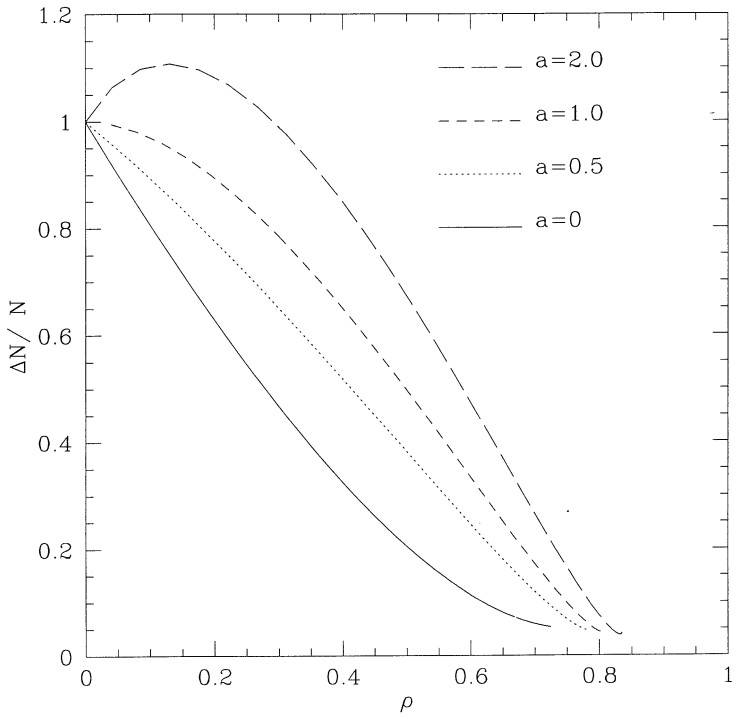

Figure 4. Fluctuations and variance of the total number of particles as functions of density for $a = 0, 0.5, 1.0, 2.0$.

particles, the adsorption process is now cooperative. Cooperativity is simply accounted for by considering that the particles interact with 'sticky-core' pair potentials [23], whose associated pair Boltzmann factor is given by

$$e(l_{12}) = e_0(l_{12}) + a\delta(l_{12} - 1) \tag{35}$$

where l_{12} is the distance between the two particle centres; the hard-core contribution, $e_0(l_{12}) = H(l_{12}-1)$, is supplemented with an attractive singular component. The probability for a new particle to be inserted at a position **1** on the line is equal to the product of all pair Boltzmann factors between the new particle in **1** and all pre-adsorbed particles. We stress that the equivalence between the ballistic deposition model and a cooperative sequential adsorption process *with pairwise additive interactions* is only valid for a one-dimensional substrate. For a two-dimensional substrate for instance, an incoming sphere can roll over four pre-adsorbed spheres before reaching the surface [11, 13], which requires one to consider a cooperative sequential adsorption process with irreversible 3-, 4-, and 5-particle interactions in addition to the pair terms.

Starting with the work of Widom [24], comparison has been made in the literature between configurations generated by random sequential addition and those at equilibrium. One-dimensional systems for which exact solutions are available in both cases have provided a detailed account of similarities and differences [15, 17, 18]. Here, we generalize these results by comparing the exact solution for the pair correlation function in the model of cooperative sequential adsorption of sticky rods with that of the equilibrium sticky-core one-dimensional fluid. The former has been given in the previous sections; the latter can

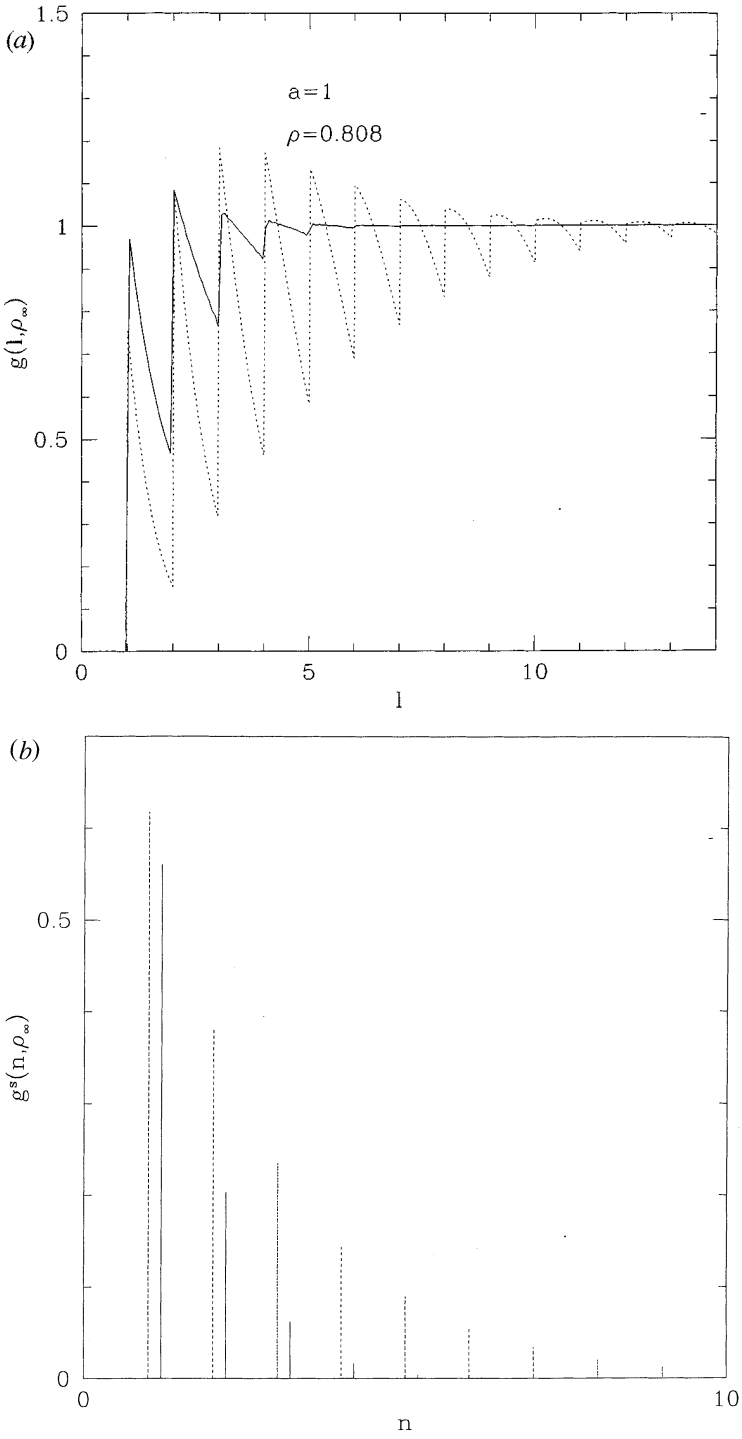

Figure 5. Comparison between the equilibrium (dashed curve) and GBD (full curve) pair correlation functions for the regular part $g(l, \rho_\infty)$ (*a*) and the singularities (*b*) $g^s(n, \rho_\infty)$ at the GBD saturation coverage for $a = 1.0$. The vertical straight lines are shifted to the right by 0.2 for the GBD model.

be obtained by using standard techniques [25, 26] and its expression in Laplace space reads

$$\rho\tilde{g}(s) = \left(\left(\frac{(\beta P + s)(1 + a\beta P)}{(1 + a\beta P + as)(\beta P)}\right) - \mathrm{e}^{-s}\right)^{-1}$$
$$= \sum_{n=1}^{+\infty} \mathrm{e}^{s}\left(\frac{(\beta P)(1 + a\beta P + as)}{(1 + a\beta P)(\beta P + s)}\mathrm{e}^{-s}\right)^{n} \tag{36}$$

or, in real space,

$$\rho g(l+1) = \sum_{n=0}^{+\infty}\left(\frac{\beta P}{1 + a\beta P}\right)^{n+1}$$
$$\times\left(a^{n+1}\delta(l-n) + \left[\sum_{m=1}^{n+1} C_{n+1}^{m}\frac{(l-n)^{m-1}}{(m-1)!}a^{n+1-m}\right]\mathrm{e}^{-\beta P(l-n)}H(l-n)\right) \tag{37}$$

with

$$\beta P = \frac{1}{2a}\left[\sqrt{1 + \frac{4a\rho}{1-\rho}} - 1\right]. \tag{38}$$

Because of the singular attractive interaction, clustering also occurs in the equilibrium fluid and the amplitudes of the singularities and discontinuities that are present at all non-zero integer values n of the distance between pairs of particles are given by

$$\rho g^{s}(n+1) = \left(\frac{a\beta P}{1 + a\beta P}\right)^{n+1} \tag{39}$$

and

$$\rho\Delta g(n+1) = (n+1)\left(\frac{\beta P}{1 + a\beta P}\right)^{n+1} a^{n}. \tag{40}$$

The long-range behaviour of the pair correlation function can be determined as follows. Equation (39) shows that the amplitudes of the singularities (and discontinuities) decrease exponentially. Therefore, correlations decay much faster in the non-equilibrium model than in the equilibrium system. Figure 5 compares the pair correlation functions of the two models for $a = 1$ at a density corresponding to saturation in the GBD case.

6. Conclusion

The generalized ballistic deposition model is an irreversible cooperative adsorption process that incorporates the effect of gravity on the deposition by means of a tuning parameter a. We have obtained an exact analytical expression for the pair distribution function, the structure factor, and the fluctuations of the number of particles. It appears that the nature of the process, for example the importance of gravity effects or the non-equilibrium features, is more clearly determined by examining the structure of the deposited layer than the kinetics or the saturation coverage. This result, whose validity certainly goes beyond one-dimensional models, can stimulate further experimental and theoretical investigations.

Acknowledgment

The Laboratoire de Physique Théorique des Liquides is Unité de Recherche Associée No 765 au Centre National de la Recherche Scientifique.

Appendix A

With the functions $X_1(s,t)$, $X_2(s,t)$, $Y_1(s,t)$, $Y_2(s,t)$, and $Y_3(s,t)$, the rate equations can be rewritten as

$$\frac{\partial \rho^2 \tilde{g}(s,t)}{\partial t} = 2h_a(t)((1+a(2t+s))X_1(s,t) + a(t+s)X_2(s,t) + ah_a(t)) \tag{A.1}$$

$$\frac{\partial}{\partial t}\begin{pmatrix} X_1 \\ X_2 \end{pmatrix} = \begin{pmatrix} -A(s,t)(1+a(t+s)) & -a(t+s)A(s,t) \\ 0 & -\frac{1}{t+s} \end{pmatrix}\begin{pmatrix} X_1 \\ X_2 \end{pmatrix} + h_a(t)\begin{pmatrix} (1+a(2t+s))Y_1 + a(t+s)Y_2 - atA(s,t) \\ (1+a(2t+s))Y_2 + a((t+s)Y_3 + \frac{t}{t+s} + (\frac{\mathrm{e}^{-s}}{t+s})C(a,t) \end{pmatrix} \tag{A.2}$$

$$\frac{\partial}{\partial t}\begin{pmatrix} Y_1 \\ Y_2 \\ Y_3 \end{pmatrix} = \begin{pmatrix} -2A(s,t)(1+a(t+s)) & -2a(t+s)A(s,t) & 0 \\ 0 & -(A(s,t)(1+a(t+s)+\frac{1}{t+s} & -(A(s,t)a(t+s)) \\ 0 & 0 & -\frac{2}{t+s} \end{pmatrix} \times\begin{pmatrix} Y_1 \\ Y_2 \\ Y_3 \end{pmatrix} + \begin{pmatrix} -B(s,t)\mathrm{e}^{-t} \\ +B(s,t)\mathrm{e}^{-t} - 2a\frac{\mathrm{e}^{-s}}{(t+s)}A(s,t)C(a,t) \\ -B(s,t)\mathrm{e}^{-t} + 2a\frac{\mathrm{e}^{-s}}{(t+s)^2}C(a,t) \end{pmatrix} \tag{A.3}$$

where we have dropped for simplicity the explicit (s,t)-dependence of the X_i's and Y_i's. We first solve the above equations for the functions Y_2, Y_3, and X_2 with the initial conditions $X_2(s,0) = 0$, $Y_2(s,0) = 1/s$, and $Y_3(s,0) = -1/s$; this leads to

$$Y_2(s,t) = -\frac{\mathrm{e}^{-t}}{t+s} \tag{A.4}$$

$$Y_3(s,t) = \frac{\mathrm{e}^{-t}}{t+s} - \mathrm{e}^{-s}\frac{C(a,t)}{(t+s)^2} \tag{A.5}$$

$$X_2(s,t) = \frac{-th_a(t)}{t+s}. \tag{A.6}$$

Then inserting equations (A.5) and (A.6) in equations (A.2) and (A.3) yields the set of equations (20)–(22).

Appendix B

We assume that any function $f(l,t)$ can be expanded as follows:

$$f(l,t) = \sum_{n=0}^{\infty}\left(\delta(l-n)\exp(-(l-n)t)f^{n,0}(t) + \sum_{m=1}^{\infty} H(l-n)(l-n)^{m-1}/(m-1)!\exp(-(l-n)t)f^{n,m}(t)\right) \tag{B.1}$$

or in Laplace space,

$$\tilde{f}(s,t) = \sum_{n=0}^{\infty}\sum_{m=0}^{\infty}\frac{\exp(-ns)}{(t+s)^m}f^{n,m}(t). \tag{B.2}$$

With this basis of functions, one can easily check that $Y_3(s,t)$, $Y_2(s,t)$, and $X_2(s,t)$ have a finite number of non-zero time-dependent coefficients: $Y_3^{0,1}(t) = \mathrm{e}^{-t}$, $Y_3^{1,2}(t) = -C(a,t)$, $Y_2^{0,1}(t) = -\mathrm{e}^{-t}$, $X_2^{0,1}(t) = -th_a(t)$.

Equations (20)–(22) can then be expressed as

$$\frac{\partial \rho^2(t) g^{n,m}(t)}{\partial t} = (m-1)\rho^2(t) g^{n,m-1}(t) + 2h_a(t)[(1+at)X_1^{n,m}(t) + aX_1^{n,m+1}(t)] \tag{B.3}$$

$$\frac{\partial X_1^{n,m}(t)}{\partial t} = (m-2)X_1^{n,m-1}(t) + \mathrm{e}^{-t}X_1^{n-1,m-1}(t) - aX_1^{n,m}(t) + a\mathrm{e}^{-t}X_1^{n-1,m}(t) + (1+at)h_a(t)Y_1^{n,m}(t) + ah_a(t)(Y_1^{n,m+1}(t) - \mathrm{e}^{-t}\delta^{0,0}) \tag{B.4}$$

$$\frac{\partial Y_1^{n,m}(t)}{\partial t} = (m-3)Y_1^{n,m-1}(t) + 2\mathrm{e}^{-t}Y_1^{n-1,m-1}(t) - 2aY_1^{n,m}(t) + 2a\mathrm{e}^{-t}Y_1^{n-1,m}(t) + (2a-1)\mathrm{e}^{-t}\delta^{0,1} + \mathrm{e}^{-t}\delta^{0,2} - 2a\mathrm{e}^{-2t}\delta^{1,1} - \mathrm{e}^{-2t}\delta^{1,2} \tag{B.5}$$

where $\delta^{\alpha,\beta}$ is a short-hand notation for the product of Kronecker symbols $\delta_{n,\alpha}\delta_{m,\beta}$.

One can now compute interval by interval the pair correlation function. The calculation becomes rapidly lengthy and we only give below the results which permit us to derive $g(l+1,t)$ for $0 \leqslant l < 1$ and $1 \leqslant l < 2$. One obtains, for $n = 0$,

$$Y_1^{0,1}(t) = \mathrm{e}^{-t} \qquad Y_1^{0,m}(t) = 0 \qquad \text{for } m \neq 1 \tag{B.6}$$

$$X_1^{0,1}(t) = th_a(t) \qquad X_1^{0,m}(t) = 0 \qquad \text{for } m \neq 1. \tag{B.7}$$

By combining these results with equation (B.3), one recovers equation (23).

For $n = 1$, one gets

$$Y_1^{1,2}(t) = C(a,t) \qquad Y_1^{1,m}(t) = 0 \qquad \text{for } m \neq 2 \tag{B.8}$$

$$X_1^{1,0}(t) = 0 \tag{B.9}$$

$$X_1^{1,1}(t) = \mathrm{e}^{-at}\int_0^t \mathrm{d}t_1\, ah_a(t_1)\mathrm{e}^{at_1}(C(a,t_1) + t_1\mathrm{e}^{-t_1}) \tag{B.10}$$

$$X_1^{1,m}(t) = \mathrm{e}^{-at}\int_0^t \mathrm{d}'t\, h_a(t_1)\mathrm{e}^{at_1}(t-t_1)^{m-2}((1+at_1)C(a,t_1) + t_1\mathrm{e}^{-t_1}) \qquad \text{for } m \geqslant 2. \tag{B.11}$$

By combining these results with equation (B.3), one recovers equation (24).

References

[1] Ramsden J 1993 *Q. Rev. Bio. Phys.* **27** 41
[2] Adamczyk Z, Siweck B, Zembala M and Belouschek P 1994 *Adv. Colloid. Surf.* **48** 151
[3] Feder J 1980 *J. Theor. Biol.* **87** 237
[4] Evans J W 1993 *Rev. Mod. Phys.* **65** 1281
[5] Ramsden J 1993 *Phys. Rev. Lett.* **71** 295
[6] Onoda G Y and Liniger E G 1986 *Phys. Rev.* A **33** 715
[7] Bafaluy J, Senger B, Voegel J-C and Schaaf P 1993 *Phys. Rev. Lett.* **70** 623
[8] Wojtaszczyk P, Schaaf P, Senger B, Zembala M and Voegel J-C 1993 *J. Chem. Phys.* **99** 7198
[9] Talbot J and Ricci S 1992 *Phys. Rev. Lett.* **68** 958
[10] Viot P, Tarjus G and Talbot J 1993 *Phys. Rev.* E **48** 480
[11] Choi H S, Talbot J, Tarjus G and Viot P 1993 *J. Phys. Chem.* **99** 9296
[12] Tarjus G, Viot P, Choi H S and Talbot J 1994 *Phys. Rev.* E **49** 3239
[13] Choi H S, Talbot J, Tarjus G and Viot P 1995 *Phys. Rev.* E **51** 1353
[14] Evans J W, Burgess D R and Hoffman D K 1984 *J. Math. Phys.* **25** 3051
[15] Evans J W 1989 *Surf. Sci.* **215** 319
[16] Monthus C and Hilhorst H J 1991 *J. Phys. A: Math. Gen.* **175** 263
[17] Pedersen F B and Hemmer P C 1993 *J. Phys. Chem.* **98** 2279
[18] Bonnier B, Boyer D and Viot P 1994 *J. Phys. A: Math. Gen.* **27** 3671
[19] Boyer D, Tarjus G, Viot P and Talbot J 1995 *J. Chem. Phys.* **103** 1607

[20] Bartelt M C and Evans J W 1994 *J. Stat. Phys.* **76** 867
[21] Tarjus G, Schaaf P and Talbot J 1991 *J. Stat. Phys.* **63** 167
[22] Schaaf P, Wojtaszczyk P, Mann E K, Senger B, Voegel J-C and Bedeaux D 1995 *J. Chem. Phys.* **102** 5079
[23] Baxter R J 1968 *J. Chem. Phys.* **49** 2770
[24] Widom B 1966 *J. Chem. Phys.* **44** 3888
[25] Percus J K 1982 *J. Stat. Phys.* **28** 67
[26] Fisher I Z 1964 *Statistical Theory of Liquids* (Chicago: The University of Chicago Press)